Molecular Structures and Potential Energy Surfaces for $IHI^-\cdot Ar_n$ ($n = 1-7$)

Ivana Adamovic and Mark S. Gordon*

Department of Chemistry, Iowa State University, Ames, Iowa 50011

Received: July 2, 2004; In Final Form: September 7, 2004

This study reports second-order perturbation (MP2) theory predictions of the optimized structures and relative energies for $IHI^-\cdot Ar_n$ ($n = 1-7$) complexes. For $n = 1-6$, the lowest energy structure has all n Ar atoms forming a partial ring in the plane that is perpendicular to and bisects the IHI^- axis. The ring is closed at $n = 6$, and for $n = 7$, one of the Ar atoms moves into a second ring. Analysis of the geometrical parameters and three-dimensional MP2 molecular electrostatic potentials (MEP) is used to determine why the ring structure is lowest in energy for $n = 1-6$, but not for $n = 7$. Based on the MEP, it is concluded that Ar atoms tend to distribute in regions of low electron density that exist in the plane perpendicular to and bisecting the IHI^- axis. Hence, the global minimum for all $n < 7$ is a ring structure in this plane. For $n = 7$, steric effects force an Ar atom into a new ring.

I. Introduction

In the last two decades, a wide range of experimental and theoretical approaches[1−7] have been developed to study chemical reaction dynamics. The most demanding task is the characterization of the transition state region. One of the most powerful experimental techniques used for this purpose is anion photodetachment.[8] In these experiments, an electron is detached from an anion whose geometry is close to that of the neutral transition state. Because the anion and neutral geometries are similar, studying the photoelectron (PE) spectrum of the anion (minimum on the potential energy surface) can provide useful information about the neutral transition state. PE spectroscopy has been used successfully in investigations of many bimolecular reactions.[4,9−14]

Since most chemical reactions take place in solution, it is of interest to investigate solvent effects[15−17] on the transition state spectroscopy and dynamics. Such a study can be accomplished by sequential addition of solvent molecules to the stable anion complex and observing clustering effects on the PE spectrum. Argon atoms are commonly chosen solvents for this purpose, since their addition to the system produces very clean PE spectra, with even better resolution of the fine spectral features, than in the solvent-free spectrum.[18,19]

The present theoretical study was inspired by the experimental work of Neumark et al.[20,21] on the $IHI^-\cdot Ar_n$ ($n = 1-15$) systems. In the first of their PE studies,[20] one Ar atom was added to an IHI^- anion. The major observations for a single Ar atom were as follows: (1) spectral shifts toward lower electron kinetic energies; (2) a prominent cooling effect caused by the reduced contribution of the vibrational hot bands to the spectral features; (3) the appearance of a new progression corresponding to IHI hindered rotation near the I+HI ($v = 1$) limit. Their second study[21] considered larger clusters, $IHI^-\cdot Ar_n$ ($n = 1-15$). An observed change in the stepwise shift after $n = 6$ was attributed to the change in the binding site of the seventh Ar atom. A change in the peak spacing between $\nu_3' = 0$ and 2 is attributed in part to a change in the IHI^- core geometry (decrease of the I−H bond). Interpretation of the experiments suggests that the lowest energy structure has the Ar atoms arranged in a ring around the waist, perpendicular to and bisecting the IHI^- axis. A similar arrangement has been observed for the $I_2^-\cdot Ar_n$ complex.[22,23] Batista and Coker,[23] using coupled quantum-classical molecular dynamics determined that the I_2^- solvation shell is built from staggered hexagonal rings of Ar atoms around the I_2^- axis. A similar conclusion was reached in another dynamic study on the $I_2^-\cdot Ar_n$ system, by Faeder et al.[22] Lavender and McCoy[7] performed dynamics calculations on the $ClHCl^-\cdot Ar_n$ complex and predicted a similar arrangement of the Ar atoms. The authors also found a slight decrease in the H−Cl distance (∼0.005 Å) as the number of Ar atoms increases; however, in their recent study on $IHI^-\cdot Ar_n$ systems, H−I bond compression has not been observed.[24]

The primary interest of this work is to investigate the $IHI^-\cdot Ar_n$ system, studied by Neumark et al., using correlated ab initio techniques. Of particular interest is to understand why Ar atoms tend to cluster in a ring structure, as found in previous studies, and why the 7th Ar atom exhibits a behavior that is different from that of the first six Ar atoms. The computational approach is presented in section II. This is followed by a presentation of the results in section III and conclusions in section IV.

II. Computational Methods

All of the calculations were performed using the GAMESS[25] electronic structure code. Geometry optimizations were obtained using second-order perturbation theory (MP2).[26] For smaller systems ($n = 1-3$), single-point energy corrections were done with the coupled cluster singles and doubles with perturbative triples (CCSD(T)[27]) method at the MP2 optimized structures. All of the stationary points were confirmed by calculating (using finite differences of analytic gradients) and diagonalizing the energy second derivative (Hessian) matrix. Because the potential energy surfaces of interest here are very flat, numerical Hessians frequently produce small imaginary frequencies. These frequencies, which are generally characterized by significant rotational contributions and very small infrared intensities, can often be removed by small changes in the step size of the numerical

* To whom correspondence should be addressed.

10.1021/jp040477n CCC: $27.50
Published on Web 11/19/2004

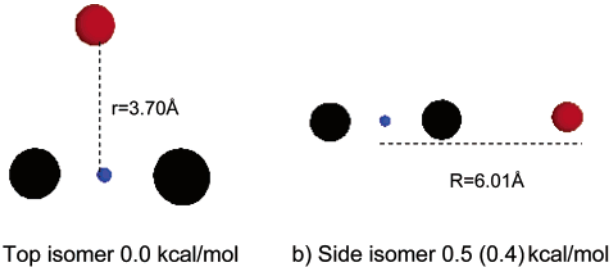

Figure 1. Isomers of $IHI^-\cdot Ar$; distances in Å, MP2 relative energies, CCSD(T) values in parentheses.

(finite differences) Hessian calculations. The global minimum for each value of n has been confirmed to have a positive definite Hessian.

Zero-point energy (ZPE) corrections were calculated using the harmonic approximation; however, due to the large number of very low-frequency modes, the harmonic analysis may not be appropriate. Therefore, the relative energies and the relative ZPEs are reported separately.

Since diffuse functions are important in describing weakly bound systems, the aug-cc-pVTZ basis set[28] was used for Ar. For I, the effective core potential (ECP) developed by Stevens et al. (SBKJC)[29,30] was used, together with the completely uncontracted SBKJC valence basis set, augmented by three sets of d (exponents = 0.120, 0.300, and 0.75) and one set of f (exponent = 0.36) functions. The hydrogen basis set is 6-311++G(2d, 2p).[31] MP2 molecular electrostatic potentials were generated and visualized using the MacMolPlt[32] program, a graphical interface for GAMESS.

III. Results and Discussion

First, geometries and relative energies of $IHI^-\cdot Ar_n$, $n = 1-7$ are presented. This is followed by a discussion of the MP2 three-dimensional molecular electrostatic potential[33] (MEP) maps, an analysis of the results, and comparison with experiments.

Note that the potential energy surfaces (PESs) of $IHI^-\cdot Ar_n$ complexes are very flat, because of the very weak interaction of the nobel gas atoms with the rest of the system. Consequently, all of the isomers for a given n are very close in energy.

The structure of the IHI^- anion stays the same for all $n = 1-7$ systems; the I−H distance is ∼1.898 Å, and the I−H−I angle is 180°.

A. $IHI^-\cdot Ar$ Complexes. Figure 1 shows the geometric parameters and relative energies for two different $IHI^-\cdot Ar$ structures. The first of these has one Ar atom in the "top" position, above the H atom, whereas the second isomer has one Ar atom in the "side" position, along the IHI^- axis. The top isomer is lower in energy by about 0.5 kcal/mol, at the MP2 level of theory, and is the global minimum for $n = 1$. Single-point CCSD(T) calculations predict the side isomer to be 0.4 kcal/mol higher, in excellent agreement with the MP2 results.

B. $IHI^-\cdot Ar_2$ Complexes. As n increases, the number of different isomers in an $IHI^-\cdot Ar_n$ complex increases. Figure 2 gives the relative energies and geometrical parameters for the four $n = 2$ isomers. The lowest energy structure (**1**, Figure 2) has both Ar atoms in the plane that is perpendicular to the IHI^- axis, with an Ar−H−Ar angle of 60.7°. This is in agreement with experiment and previous theoretical work. The next lowest energy structure (**2**, Figure 2) is a transition state in which both Ar atoms are in the same plane (perpendicular to and bisecting the IHI^- axis) but are further away from each other (7.41 vs 3.70 A) than in **1**. Clustering of Ar atoms in **1** leads to stabilization of the system and a decrease in the energy by about

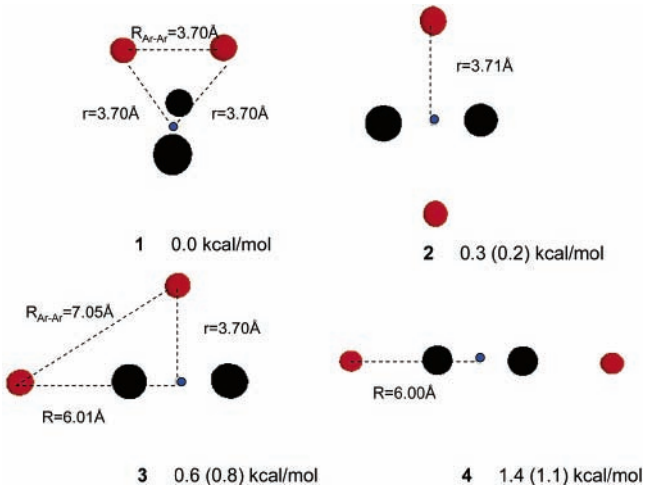

Figure 2. Isomers of $IHI^-\cdot Ar_2$; all distances in Å, MP2 relative energies (kcal/mol), CCSD(T) relative energies in parentheses.

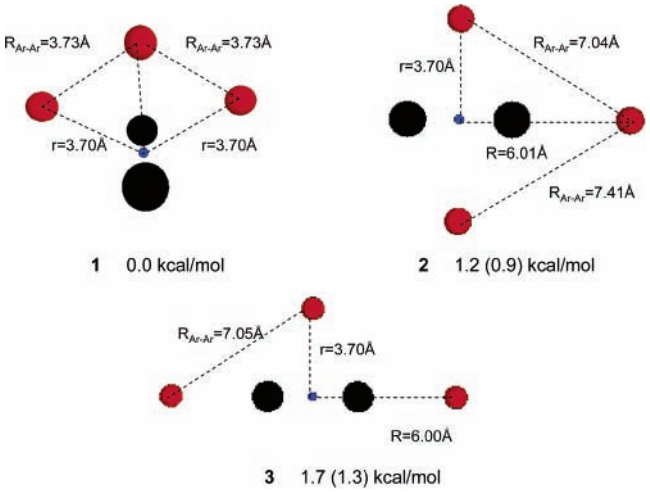

Figure 3. Isomers of $IHI^-\cdot Ar_3$; all distances in Å, MP2 relative energies (kcal/mol), CCSD(T) relative energies in parentheses.

0.3 kcal/mol. A calculation of the difference in dispersion energy, expressed in the simple London form C_6/R,[6] $C_6 = 64.3$,[34] between structures **1** and **2** leads to 0.33 kcal/mol, almost the same as the MP2 energy difference between the two structures. Attractive van der Waals forces between Ar atoms are stronger in **1**, because of the smaller Ar−Ar distance. Single point CCSD(T) energies at the optimized MP2 structures are in very good agreement with the relative MP2 energies (see Figure 2).

C. $IHI^-\cdot Ar_3$ Complexes. The relative energies and geometries for $IHI^-\cdot Ar_3$ are presented in Figure 3. All three stationary points are minima on the potential energy surface. The global minimum is structure **1**, with the partial ring of Ar atoms around the IHI^- axis (in the perpendicular plane that bisects the axis). The three Ar atoms are arranged so that the optimal ∼3.7 Å Ar−Ar distance is maintained. That is, they do not form a symmetric equilateral triangular arrangement. Structure **2** (Figure 3) with one Ar along the IHI^- axis is higher in energy than **1** by about 1.2 kcal/mol. Structure **3** has two Ar atoms along the IHI^- axis, and it is higher in energy than structure 2 by 0.5 kcal/mol. It is clear that the relative stabilities of the structures depend on the arrangement of Ar atoms: the more Ar atoms along the IHI^- axis, the higher the energy. Note that the H−Ar distance (perpendicular to the IHI^- axis) is approximately the same in all three isomers (Figure 3) and the same as in most $n = 1$ and 2 structures. Single-point energy CCSD(T) calculations were done for all isomers (Figure 3), and the biggest deviation

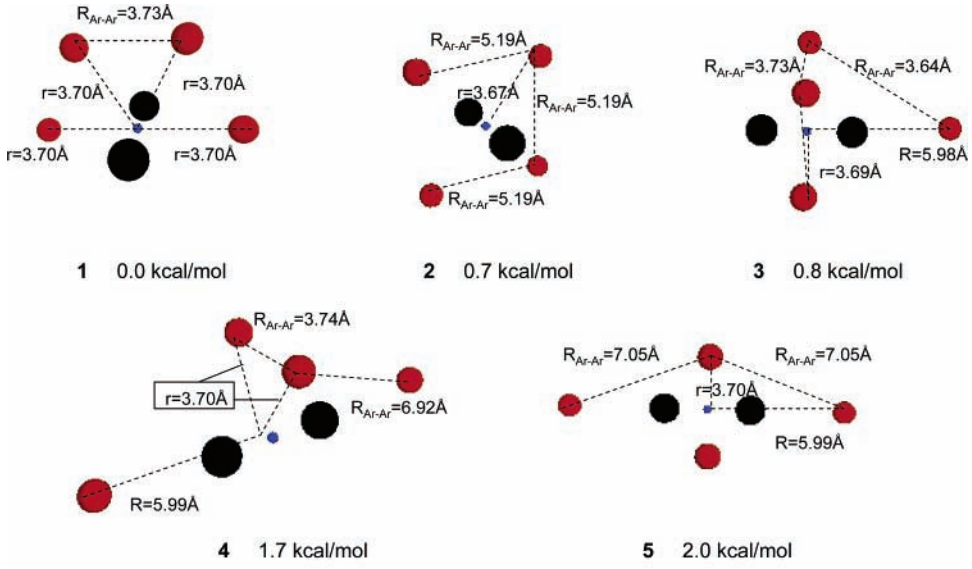

Figure 4. Isomers of $IHI^-\cdot Ar_4$; MP2 relative energies (kcal/mol), all distances in Å.

from MP2 relative energies is 0.4 kcal/mol. Since for $n = 1-3$ CCSD(T) relative energies are in good agreement with the MP2 values, for $n > 3$ systems only MP2 calculations have been performed.

D. $IHI^-\cdot Ar_4$ Complexes. The global minimum for $IHI^-\cdot Ar_4$ follows the observed trend, in which the Ar atoms are arranged in a partial ring perpendicular to and bisecting the IHI^- axis. The relative energies and bond distances for the $n = 4$ structures are summarized in Figure 4. The energy spread for the five isomers is 2.0 kcal/mol. The energy again increases when an Ar atom is moved from the ring to the axial position (on the end of the IHI^- axis) and also as the distance between adjacent Ar atoms increases (**1** vs **2** and **4** vs **5**). The energy order of the isomers is consistent with the hypothesis that the relative binding energies in these systems comes mostly from Ar clustering: increasing the distance between Ar atoms increases the relative energy of the complex. Comparing the global minimum (**1**) for $n = 4$ with $n = 1-3$ reveals that the H−Ar distance stays approximately the same (∼3.70 Å). Structure **2**, a symmetric isomer with longer Ar−Ar distances (5.19 Å vs 3.73 Å), exhibits contraction of the Ar−H distance (by 0.03 Å) as found in the $n = 4$ symmetric structure by Lavender and McCoy[7] in their study on $ClHCl^-\cdot Ar_n$ clusters. However, this symmetric structure is not the global minimum on the $IHI^-\cdot Ar_4$ potential energy surface. Rather, it is ∼0.7 kcal/mol higher in energy. As for $n = 2$, the difference in energy between **1** and **2** is due to the Ar−Ar dispersion energy.

E. $IHI^-\cdot Ar_5$ Complexes. The relative energies and distances for $IHI^-\cdot Ar_5$ are given in Figure 5. Except for the global minimum, each of these isomers has one or more imaginary frequencies in the range of 1−25 cm^{-1}, with very small intensities (0.008−0.0006 D^2/amu $Å^2$). Many of these are likely to be due to numerical noise, since they have significant contributions from rotational degrees of freedom. The lowest energy structure has all five Ar atoms in a partial ring in a perpendicular plane centered on the H atom, with an average Ar−Ar distance of 3.73 Å. This is very similar to the Ar−Ar distances in the $n = 2-4$ global minima. Structure **2** has the five Ar atoms in the same plane, but symmetrically displaced, with neighbor Ar−Ar distances of 4.23 Å. **2** is higher in energy by ∼0.3 kcal/mol, mostly due to the stronger Ar−Ar dispersion forces in **1**. Structure **2** is followed in energy by structure **3**, in which one Ar is on the IHI^- axis, whereas the fourth structure

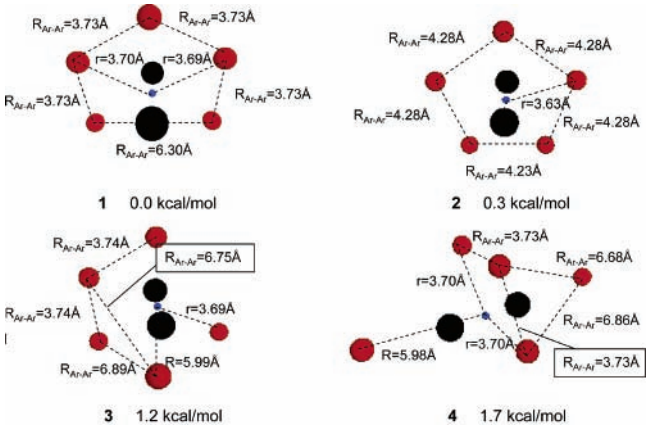

Figure 5. Isomers of $IHI^-\cdot Ar_5$; MP2 relative energies (kcal/mol), all distances in Å.

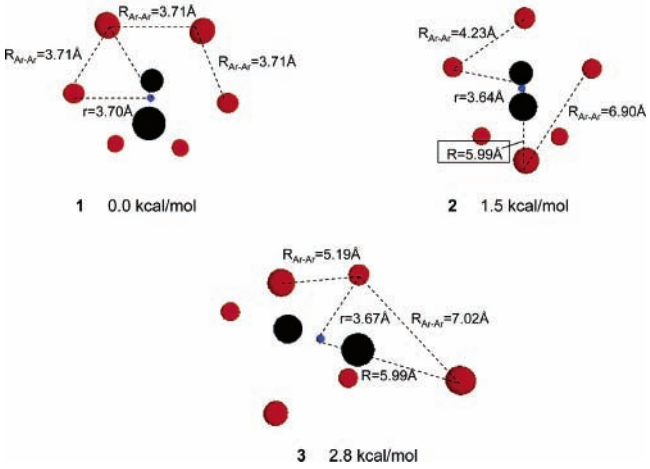

Figure 6. Isomers of $IHI^-\cdot Ar_6$; MP2 relative energies (kcal/mol), all distances in Å.

has two Ar atoms along the IHI^- axis. Note that in the $n = 5$ global minimum the Ar−H and Ar−Ar distances are the same as those in the global minima for $n = 1-4$.

F. $IHI^-\cdot Ar_6$ Complexes. The relative energies and geometric parameters for $n = 6$ are given in Figure 6. The global minimum structure for $n = 6$ has all Ar atoms in the ring around the IHI^- axis. A second structure with five Ar in the ring plane, and one

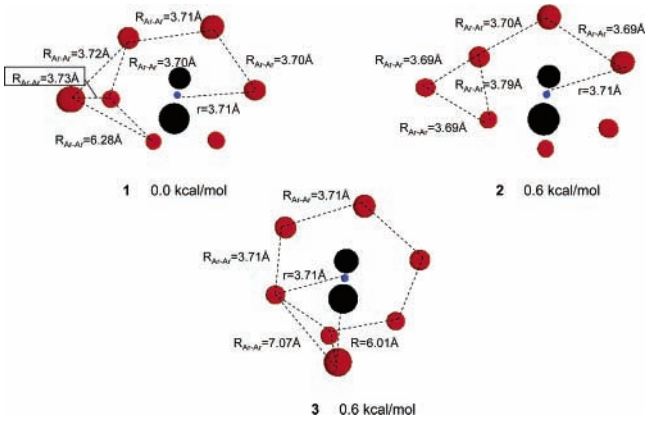

Figure 7. Isomers of $IHI^-\cdot Ar_7$; MP2 relative energies (kcal/mol), all distances in Å.

along the IHI^- axis, is higher in energy by ~1.5 kcal/mol. A third structure with energy of 2.8 kcal/mol above **1**, has one Ar atom on each end of the IHI^- axis and four Ar atoms in the ring plane. As in the case of $n = 5$, except for the global minimum, the $n = 6$ structures have very small imaginary frequencies, (1−30 cm^{-1} and intensities ~0.0007 D^2/amu-$Å^2$). The Ar−H and Ar−Ar distances in the lowest energy structure are very similar to those in the lowest energy structures for $n = 1-5$.

G. $IHI^-\cdot Ar_7$ Complexes. Geometry optimizations for $n = 7$ were initiated by choosing structures that are similar to the global minima for smaller values of n. That is, a ring of Ar atoms that bisects the IHI^- axis. In this case, however, optimization leads to a new arrangement in which six Ar atoms remain in the ring, whereas the 7th Ar moves away from the IHI^- axis. Two such structures, consistent with simulation studies on $I_2^-\cdot Ar_n$ ($n = 0-20$)[22,23] and the experimental study by Neumark et al.,[21] have been found and are shown in Figure 7. Structure **1**, in which one Ar moves out of the plane of the other six, is lower in energy by ~0.6 kcal/mol, as shown in Figure 7. The seventh Ar is positioned over one of the I atoms, so it is likely to be the first Ar in a second ring, as found in the I_2^- simulations. A third structure, in which the 7th Ar is placed in an end position, is again ~0.65 kcal/mol above structure 1. As can be seen from Figure 7, the Ar−H distances for the $n = 7$ global minimum are very similar to the $n = 6$ system, except for the 7th Ar atom, which is further away from H (5.08 Å vs 3.71 Å). Structure **2** has two groups of distances, one shorter (3.69 Å vs 3.71 A) and one the same as in structure 1; the 7th Ar atom is in the same plane as the other six and much further away, ~ 6.39 Å. In the third structure, the distance of the 7th (end) Ar atom from the H is ~6.01 Å, as in the $n < 7$ systems.

In the $n = 7$ global minimum structure, the nearest neighbor Ar−Ar distance is again on average 3.73−3.71 Å. It seems that an Ar−Ar distance of ~3.7 Å balances attractive Ar−Ar van der Waals forces and repulsion of their electron densities and gives rise to particularly stable structures.

Table 1 summarizes the binding energy, E_b, and binding energy per Ar atom, $\bar{E}_b$ for all of the global minimum isomers for $n = 1-7$. For smaller systems, $n = 1-3$, CCSD(T) binding energies were calculated and the agreement with MP2 binding energies is satisfying. Both E_b and $\bar{E}_b$ increase monotonically for $n = 1-6$. The global minimum for $n = 6$ has the largest $\bar{E}_b$, so it is a particularly stable structure. For $n = 7$, there are two groups of Ar atoms: six equivalent Ar atoms in the ring plane and a 7th Ar atom, which apparently starts a new ring. Since the inner shell for $n = 7$ is the same in structure as that for $n = 6$, it can be assumed that the first six Ar atoms have the same binding as in $n = 6$. For the 7th Ar atom the differential binding energy is calculated as the difference between the total energies for $n = 7$ and 6. The differential binding energy for the 7th Ar atom is 0.88 kcal/mol, almost two times smaller than $\bar{E}_b$ for $n = 6$. The 7th Ar atom is much further away from the IHI^- complex, and it is above the negatively charged I^-, so this result is not surprising.

TABLE 1: Total Binding Energy and Binding Energy/Ar Atom (kcal/mol) for Global Minima Structures

n	E_b[a]	$\bar{E}_b$[b]
1	1.32 (1.09)[d]	1.32 (1.09)[d]
2	2.96 (2.41)[d]	1.48 (1.20)[d]
3	4.59 (3.74)[d]	1.53 (1.25)[d]
4	6.24	1.56
5	7.93	1.59
6	9.90	1.65
7		0.88[c]

[a] $E_b = E(n\mathrm{Ar} + IHI^-) - E(IHI^-\cdot Ar_n)$. [b] $\bar{E}_b = E_b/n$. [c] Differential binding energy for the 7th Ar atom (energy difference between structures 1 for $n = 6$ and 7). [d] Numbers in parentheses are CCSD(T) values.

TABLE 2: Relative ZPE Corrections (kcal/mol) for $n = 1-7$

	ZPE
$n = 1$	−0.02
$n = 2$, structure 2	−0.04
$n = 2$, structure 3	−0.07
$n = 2$, structure 4	−0.09
$n = 3$, structure 2	−0.14
$n = 3$, structure 3	−0.12
$n = 4$, structure 2	−0.24
$n = 4$, structure 3	−0.21
$n = 4$, structure 4	−0.28
$n = 4$, structure 5	−0.32
$n = 5$, structure 2	−0.12
$n = 5$, structure 3	−0.12
$n = 5$, structure 4	−0.16
$n = 6$, structure 2	−0.24
$n = 6$, structure 3	−0.30
$n = 7$, structure 2	−0.04
$n = 7$, structure 3	−0.06

H. ZPE Corrections. The relative energies reported above have not been corrected for ZPEs, because the harmonic approximation is inappropriate for the treatment of species with many very low-frequency vibrational modes. For reference, the relative harmonic ZPE corrections are summarized in Table 2. These ZPE corrections are all very small. So, they have no qualitative impact on the discussion presented above.

I. Analysis of the MP2 Molecular Electrostatic Potentials (MEPs). Experiments and theory agree that the global minima for $IHI^-\cdot Ar_n$ $n = 1-6$ have the n Ar atoms in a ring in a plane perpendicular to and bisecting the IHI^- axis, whereas the 7th Ar appears to be in a second ring, around the IHI^- axis. This could be due to a steric effect (i.e., seven Ar atoms cannot fit in the ring around the IHI^-) or there may be electronic effects. To explore this issue, as well as to understand the reason Ar atoms cluster in a ring about the IHI^- "waist", the three-dimensional MP2 MEP was explored.

A three-dimensional map of the molecular electrostatic potential provides basic information on the distribution of electrostatic interactions in molecular systems. Although interactions such as dispersion cannot be addressed using MEP maps, an analysis of the electrostatic potential can provide useful information on the primary bonding in these systems.

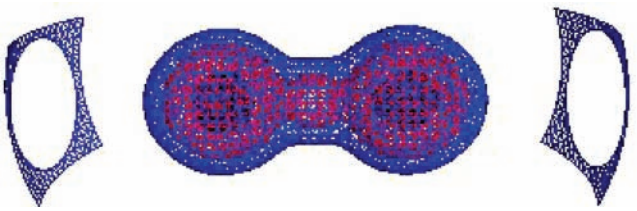

Figure 8. Molecular electrostatic potential (MEP) maps for IHI^-.

Since the same trend is observed in the MEP maps for all n, the MEP map analysis is presented only for $n = 0$, 2, and 5. Conclusions based on these systems are generally applicable to all *n*. The MEP is defined as a potential of molecular density felt by a +1 charge, evaluated over a certain number of grid points ($30 \times 30 \times 30$). For reference, the unsolvated MEP for IHI^- is given in Figure 8. Positive and negative regions of charge density are represented in red and blue, respectively. Note that directly above the H atom there is a hollow in the potential, in which an Ar could fit. Figure 9 shows the 3-dimensional MP2 MEP map for four $n = 2$ structures. Structures **1** and **2** have much smaller repulsion between the Ar electron density clouds (blue area around red positive Ar nuclei) and the negative charge of the IHI^- (blue area around IHI^-) than **3** and **4**. In the first two structures, both Ar atoms are in a region that is "density deficient" (in the plane bisecting the IHI^- axis). Hence, they feel repulsion from negative (blue) IHI^- density (concentrated mostly on the iodines) much less than Ar atoms that are located at the ends of the IHI^- axis. Structure **3** has one Ar atom in the electron density deficient region and one close to the negative (blue) iodine end. So, it is higher in energy than structures **1** and **2**, but lower than **4**, which has both Ar atoms in end positions, where most of the negative charge is concentrated. In the first two structures there is a protrusion (bump) of Ar electron density in a hollow of the negative charge of IHI^-. In **3** and **4**, the Ar electron density bump is just opposite to a similar IHI^- bump, causing increased repulsion.

The main $n = 2$ features are also present in Figure 10 for $IHI^-\cdot Ar_5$. Structures **1** and **2**, with all five Ar atoms in ring positions, are the lowest in energy because of the smallest repulsion between Ar electron density and the IHI^- negative charge. Structure **3** has one Ar atom in a side position, close to the IHI^- negative charge, whereas **4** has two Ar atoms along the IHI^- axis and therefore the greatest repulsion. Hence, the energy of $IHI^-\cdot Ar_5$ isomers increases on going from **1** to **4**.

Now, we consider the structural change upon going from $n = 6$ to 7. The Ar van der Waals radius[35] is 1.91 Å. Table 3 gives the averaged H−Ar distances for the global minima for $IHI^-\cdot Ar_n$, $n = 1-6$ systems. For $n = 1$, this distance is 3.7003 Å. As *n* increases, *r* gradually decreases reaching a minimum at $n = 4$ and 5 of 3.6957 A. For $n = 6$, *r* increases to 3.7097Å. The circumference of a ring calculated from these distances for $n = 1$ is 23.2379 Å. This decreases to 23.2090 Å for $n = 4$ and 5 and then increases to 23.2975 Å for $n = 6$. If the circumference for $n = 6$ is divided by the number of Ar atoms and then halved, one gets 1.94 Å, which is very close to the van der Waals radius of Ar. If this circumference is divided by 7 and then halved, the result is 1.6641 Å, much smaller than the Ar van der Waals radius. This simple geometrical analysis illustrates the importance of steric effects on the arrangement of Ar atoms.

One might also consider Ar−Ar electron repulsion. It is possible that excess electron density on the Ar atoms, from the negative IHI^- complex, could enhance Ar−Ar repulsion. To test this possibility, Mulliken charges were determined for the $n = 1-6$ global minima. Most of the negative charge, however, is located on the iodines for all *n*. Therefore, Ar−Ar repulsion due to charge transfer is apparently not a major factor in determining the size of the first solvation shell.

Figure 11 shows a 3-D MP2 MEP map for the $n = 6$ global minimum. Comparing this with **1** in Figure 10, it is clear that the negative regions of the Ar−Ar densities are much closer to each other in $n = 6$ than in $n = 5$. Ar−Ar repulsion increases as *n* increases from 5 to 6, because more electron density is "packed" into almost the same volume. It seems that repulsion

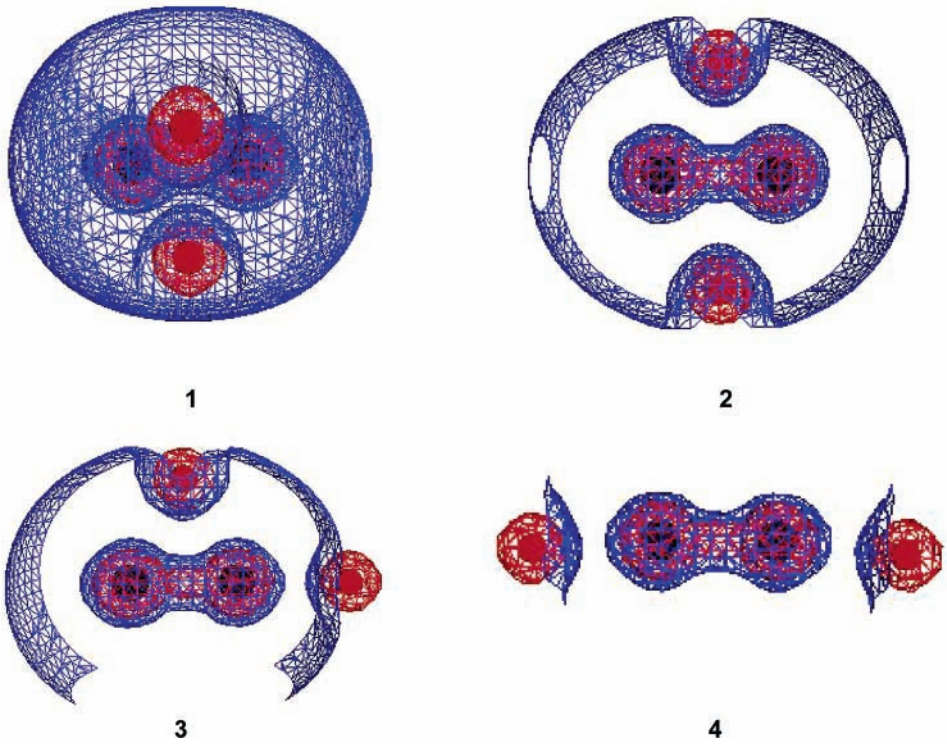

Figure 9. Molecular electrostatic potential (MEP) maps for $IHI^-\cdot Ar_2$.

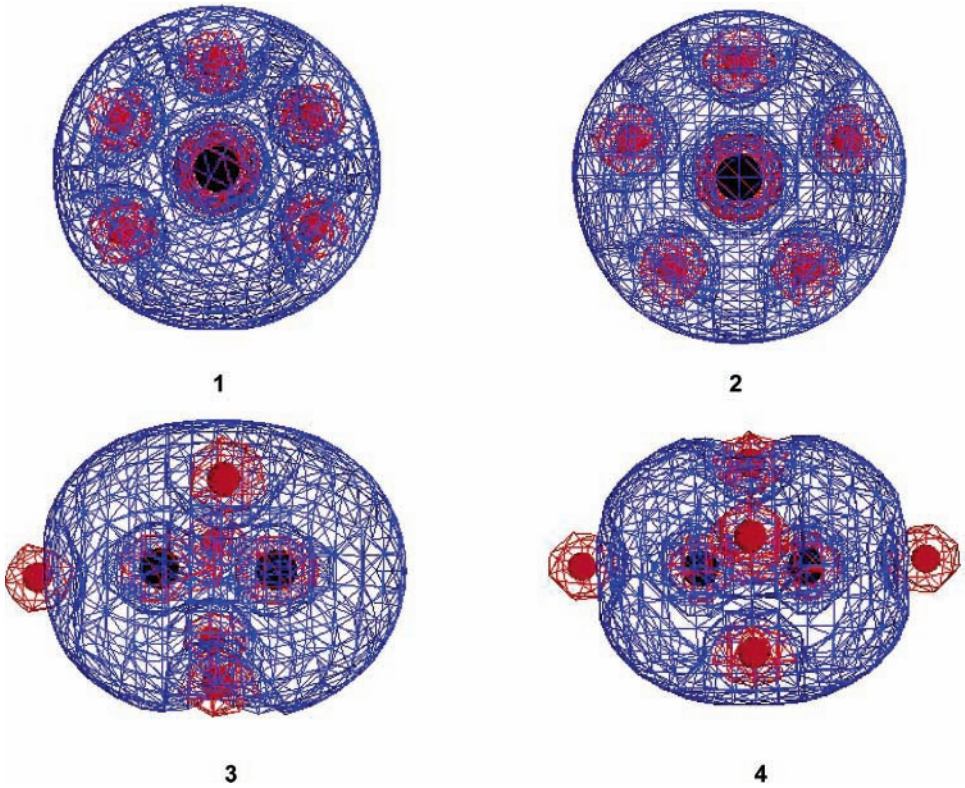

Figure 10. Molecular electrostatic potential (MEP) maps for $IHI^{-}\cdot Ar_5$.

TABLE 3: Averaged H−Ar Distance (Å) in the Lowest Energy Structures for $n = 1-7$ $|H|^{-}\cdot Ar_n$

n	r^a	*n*	r^a	*n*	r^a
1	3.7003	3	3.6985	5	3.6957
2	3.6996	4	3.6957	6	3.7098

[a] H−Ar distance perpendicular to the $|H|^{-}$ axis.

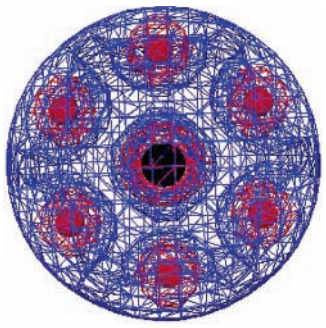

Figure 11. Molecular electrostatic potential (MEP) map for structure **1** of $IHI^{-}\cdot Ar_6$.

of the electron density increases for $n = 6$ and becomes larger than the van der Waals forces when $n = 7$. This may enhance the migration of the 7th Ar atom from the ring.

J. Vertical Detachment Energies (VDEs). One of the important experimental observations is the successive shift of the photoelectron spectrum toward lower electron kinetic energies with larger cluster size. This was attributed to the different interaction strengths of the Ar atoms with the neutral and anionic complex, namely the difference between weak van der Waals and stronger charge-induced dipole interaction.[21]

In this study, VDEs were calculated as the difference in energy between the anionic IHI^{-} complex and neutral IHI, at optimized anion geometries. The VDE and relative shifts in VDE (ΔVDE), together with experimental VDE and ΔVDE, are reported in Table 4. Both absolute values of VDE and the relative shifts (ΔVDE) are in very good agreement with the experimental values. The biggest difference is ~3 mEV for the absolute VDE n = 3. This excellent agreement confirms the experimental observation that the origin of successive shifts is due to the stronger stabilization of the anionic vs neutral complex with the addition of new Ar atoms to the system. Also, the abrupt change of the ΔVDE for n = 7 suggests different binding site for the 7th Ar atom, as discussed above.

TABLE 4: Vertical Detachment Energies (VDE, eV) and Shifts in the VDE (ΔVDE, meV) of $IHI^{-}\cdot Ar_n$ Clusters

n	1	2	3	4	5	6	7
$VDE^{exp\,a}$	20	41	63	81	100	118	130
ΔVDE^{exp}	20	21	19	18	19	18	13
VDE	20	40	60	80	100	120	130
ΔVDE	20	20	20	20	20	20	10

[a] Experimental VDEs and ΔVDE taken from ref 21.

IV. Conclusions

MP2 optimizations were performed on $IHI^{-}\cdot Ar_n$, with $n = 1-7$. For all of the systems up to $n = 6$, the lowest energy structure has *n* Ar atoms forming a ring in the plane perpendicular to and bisecting the IHI^{-} axis. This type of structure is the most stable because it has the smallest repulsion between negatively charged iodines and the Ar density. Additional stabilization comes from the Ar−Ar clustering effect, due to the dispersion interaction. The Ar−Ar distance of ~3.70−3.73 Å (that occurs in all of the global minima structures) maximizes the Ar−Ar dispersion interaction. This observed distance is in agreement with the Ar−Ar equilibrium distance in the Ar dimer (3.75 Å).[34] This finding suggests that the final stabilization in the system depends only on the arrangement of Ar atoms between each other; hence, it is determined by the Ar−Ar dispersion interaction.

Experiments suggest that the 7th Ar atom does not bind in the ring structure. This is supported by the MP2 calculations

presented here. The lowest energy structure for $n = 7$ has six Ar atoms in the ring, whereas the seventh Ar atom leaves the first ring. The most probable reason for this is a steric effect that induces Ar−Ar repulsion due to close packing.

The calculations reported here are in general agreement with the dynamics study of $ClHCl^-\cdot Ar_n$, by Lavender and McCoy. For $n = 1-3$, the predicted global minima are very similar. However, for $n = 4$ and 5, Lavender and McCoy predict a ring of Ar atoms in which the Ar atoms are symmetrically displaced in a square and pentagon, respectively. The MP2 calculations reported here, in contrast, predict that Ar atoms prefer to cluster asymmetrically in order to maximize the stabilization due to dispersion. The symmetric arrangement does not occur until $n = 6$, for which the Ar−Ar distances correspond to the ideal values for the dispersion interaction. It is likely that a method that includes dispersion is necessary to capture this effect.

Acknowledgment. The authors are grateful to Professor Daniel Neumark for suggesting this research and for many valuable discussions. This work has been supported by a grant from the Air Force Office of Scientific Research. The calculations in this work were performed in part on an IBM workstation cluster made possible by grants from IBM in the form of a Shared University Research grant, the United States Department of Energy, and the United States Air Force Office of Scientific Research and in part on the Cray T3E at the Army High Performance Computational Research Center.

References and Notes

(1) Zewail, A. H. *Science* **1988**, *242*, 1645.
(2) Schatz, G. C. *J. Phys. Chem.* **1990**, *94*, 6157.
(3) Neumark, D. M. *Ann. Rev. Phys. Chem.* **1992**, *43*, 153.
(4) Manolopoulos, D. E.; Stark, K.; Werner, H. J.; Arnold, D. W.; Bradforth, S. E.; Neumark, D. M. *Science* **1993**, *262*, 1852.
(5) Polanyi, J. C.; Zewail, A. H. *Acc. Chem. Res.* **1995**, *28*, 119.
(6) Schatz, G. C. *J. Phys. Chem.* **1996**, *100*, 12839.
(7) Lavender, H. B.; McCoy, A. B. *J. Phys. Chem. A* **2000**, *104*, 644.
(8) Neumark, D. M. *Acc. Chem. Res.* **1993**, *26*, 33.
(9) Weaver, A.; Metz, R. B.; Bradforth, S. E.; Neumark, D. M. *J. Phys. Chem.* **1988**, *92*, 5558.
(10) Bradforth, S. E.; Weaver, A.; Arnold, D. W.; Metz, R. B.; Neumark, D. M. *J. Chem. Phys.* **1990**, *92*, 7205.
(11) Metz, R. B.; Weaver, A.; Bradforth, S. E.; Kitsopoulos, T. N.; Neumark, D. M. *J. Phys. Chem.* **1990**, *94*, 1377.
(12) Waller, I. M.; Kitsopoulos, T. N.; Neumark, D. M. *J. Phys. Chem.* **1990**, *94*, 2240.
(13) Weaver, A.; Metz, R. B.; Bradforth, S. E.; Neumark, D. M. *J. Chem. Phys.* **1990**, *93*, 5352.
(14) Arnold, D. W.; Xu, C.; Neumark, D. M. *J. Chem. Phys.* **1995**, *102*, 6088.
(15) Arnold, D. W.; Bradforth, S. E.; Kim, E. H.; Neumark, D. M. *J. Chem. Phys.* **1995**, *102*, 3510.
(16) Arnold, D. W.; Bradforth, S. E.; Kim, E. H.; Neumark, D. M. *J. Chem. Phys.* **1995**, *102*, 3493.
(17) Yourshaw, I.; Zhao, Y.; Neumark, D. M. *J. Chem. Phys.* **1996**, *105*, 351.
(18) Asmis, K. R.; Taylor, T. R.; Xu, C.; Neumark, D. M. *J. Chem. Phys.* **1998**, *109*, 4389.
(19) Ayotte, P.; Weddle, G. H.; Kim, J.; Johnson, M. A. *Chem. Phys.* **1998**, *239*, 485.
(20) Liu, Z.; Gomez, H.; Neumark, D. M. *Chem. Phys. Lett.* **2000**, *332*, 65.
(21) Liu, Z.; Gomez, H.; Neumark, D. M. *Faraday Discuss.* **2001**, *118*, 221.
(22) Faeder, J.; Delaney, N.; Maslen, P. E.; Parson, R. *Chem. Phys. Lett.* **1997**, *270*, 196.
(23) Batista, V. S.; Coker, D. F. *J. Chem. Phys.* **1997**, *106*, 7102.
(24) McCoy, A. B. private communication, 2004.
(25) Schmidt, M. W.; Baldridge, K. K.; Boatz, J. A.; Elbert, S. T.; Gordon, M. S.; Jensen, J. H.; Koseki, S.; Matsunaga, N.; Nguyen, K. A.; et al. *J. Comput. Chem.* **1993**, *14*, 1347.
(26) Moller, C.; Plesset, S. *Phys. Rev.* **1934**, *46*, 618.
(27) Piecuch, P.; Kucharski, S. A.; Kowalski, K.; Musial, M. *Comput. Phys. Commun.* **2002**, *149*, 71.
(28) Woon, D. E.; Dunning, T. H., Jr. *J. Chem. Phys.* **1993**, *98*, 1358.
(29) Stevens, W. J.; Krauss, M.; Basch, H.; Jasien, P. G. *Can. J. Chem.* **1992**, *70*, 612.
(30) Cundari, T. R.; Stevens, W. J. *J. Chem. Phys.* **1993**, *98*, 5555.
(31) Krishnan, R.; Binkley, J. S.; Seeger, R.; Pople, J. A. *J. Chem. Phys.* **1980**, *72*, 650.
(32) Bode, B. M.; Gordon, M. S. *J. Mol. Graphics Mod.* **1998**, *16*, 133.
(33) Politzer, P., Truhlar, D. G., Eds.; *Chemical Applications of Atomic and Molecular Electrostatic Potentials. Reactivity, Structure, Scattering, and Energetics of Organic, Inorganic, and Biological Systems*; Plenum Press: New York, 1981.
(34) Stone, A. J.; *The Theory of Intermolecular Forces*; Clarendon Press: Oxford, U.K., 1996.
(35) Emsley, J. *The elements*; Oxford University Press: New York, 1989.